IMPROVED FLOODING EXPERIMENTS IN HETEROGENEOUS ROCKS USING IN-SITU SATURATIONS FROM X-RAY CT MEASUREMENTS

Svein Håvard Midtlyng and Jan Åge Stensen, Statoil Research Centre

Abstract

The improvement of core flooding experiments by measuring in-situ saturations in addition to standard effluent production has in many cases been of great importance for correct interpretation of the experiments. Some actual experimental cases have been selected to demonstrate the additional information obtained from the saturation measurements. A general recommendation from this work will be to include in-situ saturation measurements when using heterogeneous rocks and in cases where complex 3-phase core floods are performed. Depending on the knowledge of rock material (heterogeneity) and what flooding process to be studied, proper 1-D or 2-D in-situ method should be applied.

Introduction

X-ray computer tomography (CT) techniques have been applied [1,2] for quite some time to enhance the information from core flooding experiments. X-ray scans of dry core samples have often been used for the selection of proper homogeneous cores. Most flooding experiments are still performed in a way where only effluent production and pressures are measured. When in-situ measurements are included, average cross-sectional measurements are most commonly performed, anticipating the core flood to be true 1-dimentional. Such measurements may reveal saturation gradients along the core at initial, at residual or at steady state conditions. These effects may be caused by several reasons, the fluid initialization procedure, capillary end effects, limited fluid contact for composite cores, cross-sectional layering (heterogeneities) or gravity effects for vertical floods. For these cases, 1-D in-situ saturations may be sufficient for the interpretation of the experiments. In other cases, 2-D saturation information are, however, needed for a correct interpretation of the flood. Heterogeneities may in general influence the fluid flow in all three dimensions. Flow barriers may in general be identified observing the flow behaviour in the rock (core or slab). The observation of gravity effects in horizontal floods are also examples where 2-D saturation measurements are needed.

The following cases of CT-surveyed flooding experiments are discussed briefly:
i) homogeneous cores, ii) heterogeneous cores, iii) heterogeneous rock slabs, iv) 3-phase reservoir condition core floods. Some details about the experimental method are also presented.

Experimental method

The flooding experiments were performed using a dual energy Siemens Somaton DRH medical CT scanner. It is a third generation scanner, where the energy level can be changed from 90-125 kV_{peak}. A Silicon Graphics workstation was used for the image analysis.

For 2-phase flow experiments, the contrast in CT signal between oil and water phase was enhanced by adding a dopant (NaI) to the water phase. The formulas for calculating 2- phase saturations (Eq. 2,3) when doing flooding experiments in porous media can be solved from Eq. (1).

$$CT_x = CT_w S_w + CT_o S_o \qquad (1)$$
$$S_w = (CT_x - CT_o) / (CT_w - CT_o) \qquad (2)$$
$$So=1-Sw \qquad (3)$$

CT_x: CT image of core at a given saturation of water/oil
CT_w: CT image of 100% water saturated core
CT_o: CT image of 100% oil saturated core
S_w: water saturation
S_o: oil saturation

For 3-phase experiments, the dual energy mode was used, and dopants were added to both water ($Na_2WO_4*2H_2O$) and oil (iododecane). Signal/noise ratio is less when using dual energy than single energy mode for 2-phase calculations. The amount of dopants added was obtained from an optimization procedure represented by a 3-phase triangle, showing the resulting CT numbers from scanning at low and high energy for 100 % saturation of water, oil and gas, respectively. The fluids including dopants were equilibrated prior the experiment to assure thermal equilibrium. The CT numbers for scanning at two energy levels are given in Eq. (4) and (5).

$$CT_{x1} = CT_{w1} S_w + CT_{o1} S_o + CT_{g1} S_g \qquad (4)$$
$$CT_{x2} = CT_{w2} S_w + CT_{o2} S_o + CT_{g2} S_g \qquad (5)$$
$$S_w + S_o + S_g = 1 \qquad (6)$$

Solving these equations gives:

$$S_w = \frac{CT_{x1}(CT_{o2}-CT_{g2}) + CT_{x2}(CT_{g1}-CT_{o1}) + CT_{o1}CT_{g2} - CT_{g1}CT_{o2}}{CT_{w1}(CT_{o2}-CT_{g2}) + CT_{w2}(CT_{g1}-CT_{o1}) + CT_{o1}CT_{g2} - CT_{g1}CT_{o2}} \qquad (7)$$

$$S_o = \frac{CT_{x1}(CT_{w2}-CT_{g2}) + CT_{x2}(CT_{g1}-CT_{w1}) + CT_{w1}CT_{g2} - CT_{g1}CT_{w2}}{CT_{o1}(CT_{w2}-CT_{g2}) + CT_{o2}(CT_{g1}-CT_{w1}) + CT_{w1}CT_{g2} - CT_{g1}CT_{w2}} \qquad (8)$$

CT_{xi}: CT image of core at a given saturation of water/oil/gas
CT_{wi} : CT image of 100% water saturated core
CT_{oi} : CT image of 100% oil saturated core
CT_{gi} : CT image of 100% gas saturated core
i=1: low energy; i=2: high energy

Experimental cases

The selected experiments are presented below, and examples of CT saturations are given.

i) Homogeneous core. In-situ fluid saturations were used to evaluate the oil/water relative permeability measurements by the steady state method (SS). The selection of a homogeneous core was based on CT-scan of dry core, from porosity map calculated from CT-data and by CT-surveilled miscible displacement experiment. If the fluid distribution during the SS experiment was not uniform, it had to be caused by experimental method and not by heterogeneities in the sample. Fig. 1 shows water saturation profiles from both drainage and imbibition process. The saturation was fairly uniform during imbibition and drainage, only the last step in the drainage showed a clear profile caused by capillary end effects. A saturation image from the imbibition cycle (Fig. 2) is showing a fairly uniform saturation, although a limited saturation gradient close to the outlet may be observed. Relative permeabilities were found to be valid, except for the endpoint drainage value.

ii) Heterogeneous core. Oil/water relative permeability measurements of heterogeneous rock samples (hammocky cross bedded) were performed. Fig. 3 gives the porosity distribution of a cross-section, showing typical laminations in the core. Two twin core samples were tested, one by SS and the other by unsteady state (USS) method. The laminations were oriented along the main flow direction, and the injection was performed with core oriented in vertical position. The flooding behaviour was monitored by CT scanning in one longitudinal section. The saturation was also calculated in 5 cross sections at each endpoint. The results showed that the saturation profiles during SS flow conditions were fairly uniform, a strong saturation gradient was, however, observed at the water flood endpoint. Water saturations showed large variations within a cross section, typically from 0.1 to 0.4 after drainage, and between 0.5 and 0.8 after water flooding (Fig. 4). The measured SS relative permeabilities were used as input for further upscaling.

iii) Heterogeneous rock slab. Sequences of flooding experiments in a heterogeneous rock slab (10cm x10cm x 2cm) were performed to evaluate the effect of layering on the flooding performance. The rock slab size was limited to approximately 10cmx10cm when doing longitudinal scanning due to the strong attenuation of X-ray signal. Prior to flooding, the rock slab was characterized by a minipermeameter, measuring the air permeability on the rock surface in the requested grid (Fig. 5). A miscible flooding at 100% water saturation was performed. The displacement is visualized in Fig. 6, where a fingering pattern was caused by the permeability contrasts according to Fig. 5. Irreducible water saturation was established by oil flooding. CT-measurements showed large variations of initial water saturation according to permeability, high water saturation in the low permeability layers and vice versa. The water flooded residual oil distribution was found to be more uniform. A tertiary gas (nitrogen) injection produced additional oil, mainly from the high permeability zones (Fig. 7). By prolonged gas flooding, additional liquid (water and oil) was produced by evaporation, giving relatively high gas saturations even in the low permeability zones.

Table 2. Region properties as shown in Fig. 5.

	Region 1	Region 2
Permeability (mD)	650	240
Sw - after drainage	0.236	0.331
Sw - after water injection	0.517	0.523
Sg - after gas injection	0.665	0.417
Sg - after 2. water injection	0.302	0.238

Finally, the experiment was terminated with a second water flood, giving a distribution of trapped gas saturation, but no further oil production was observed. Table 2 summarizes average endpoint saturations for a high- and a low permeability region, defined in Fig. 5. Calculation of phase saturations from mass balance (production) gave good agreement to saturation CT-data, except for the gas flood due to erroneous mass balance because of evaporation.

iv) Three-phase reservoir condition core floods. Flooding experiments were performed under reservoir conditions (temperature=100 °C, pressure=300 bar) on a restored reservoir core with in-situ 3-phase saturation measurements. Gas and oil injections at irreducible water saturation as well as water-alternating-gas (WAG) injection schemes were carried out (see [3] for details). The core was oriented vertically during flooding, but turned horizontally during CT measurements in six cross sections along the core, normally after each flooding sequence. Average oil saturation during the first part of the WAG injection is given in Fig. 8. An anomalous high irreducible water saturation was measured at relative position 0.1, probably due to the fluid initialization procedure (centrifuge). The saturation profiles shown in Fig. 8 are illustrating that there might be significant changes without any oil production. A waterflood was followed by a (tertiary) gas injection displacing an "oil bank" towards the outlet, but the end effect kept the oil saturation high at the outlet. Mass balance calculations when doing several sequences of complex floods will give inaccurate saturations, and in-situ saturation measurements may in general be necessary.

Conclusions

- X-ray CT measurements during core floods may give fast and accurate in-situ saturations.
- Even for homogeneous cores, saturation gradients may give erroneous relative permeability measurements if neglected.
- Detailed saturation measurements of heterogeneous rocks may be used for more detailed interpretation of core floods.
- When doing core experiments including complex flooding schemes, in-situ saturations may be necessary for proper understanding of the experiment.

References

[1] Hove, A.O., Ringen, J.K. and Read, P.A.:"Visualization of Laboratory Corefloods With the Aid of Computerized Tomography of X-Rays", SPERE, 1987.
[2] Vinegar, H. J., Wellington, S. L.:"Tomographic imaging of three-phase flow experiments", Rev. Sci. Instrum. 58 (1), January 1987, 96-107.
[3] Akervoll I., Talukdar M.S., Midtlyng S.H., Torsæter O. and Stensen J.A.:"WAG Injection Experiments With CT In-Situ Saturation Measurements at Reservoir Conditions and Simulations",SPE /DOE Improved Oil Recovery Symposium, Tulsa, 2000, SPE 59323.

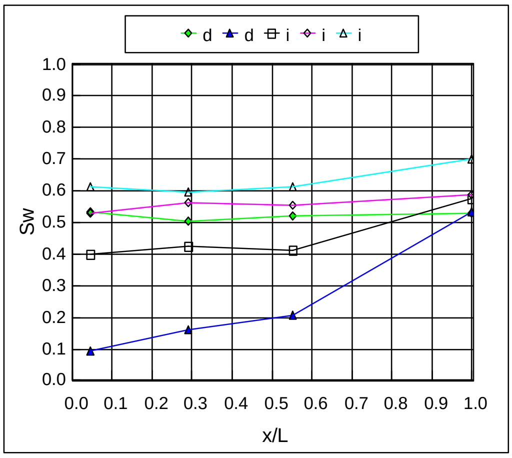

Fig. 1. Water saturation profiles during SS test, drainage (d) and imbibition (i).

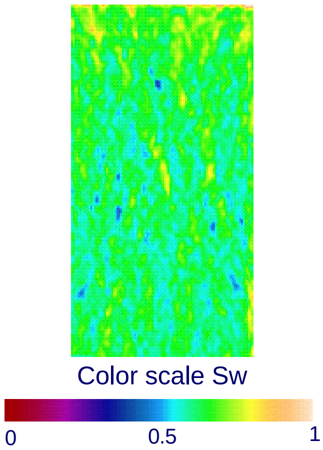

Fig. 2. Water saturation in longi-tudinal section from imbibition floodi
Sw=0.62

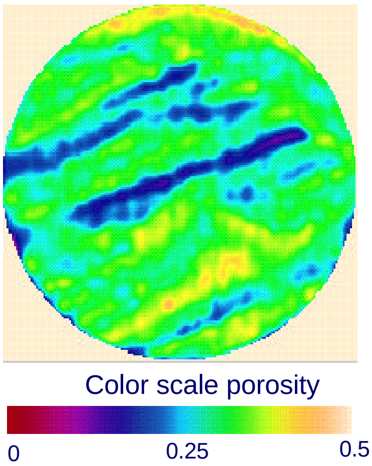

Fig. 3. Porosity map in cross section no. 3 calculated from CT data .

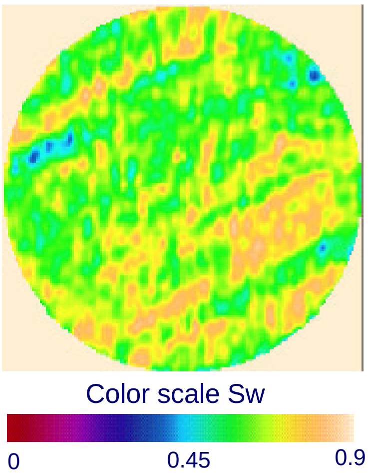

Fig. 4. Water saturation in cross section no. 3 after water flooding.

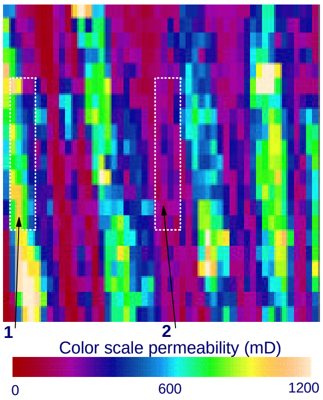

Fig. 5. Rock slab permea-bility map with regions defined.

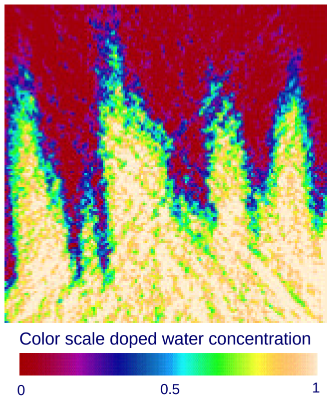

Fig. 6. Visualization of miscible water injection.

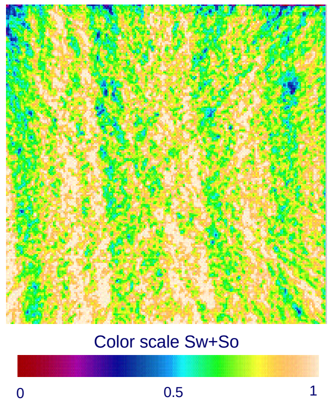

Fig. 7. Visualization of tertiar gas injection.

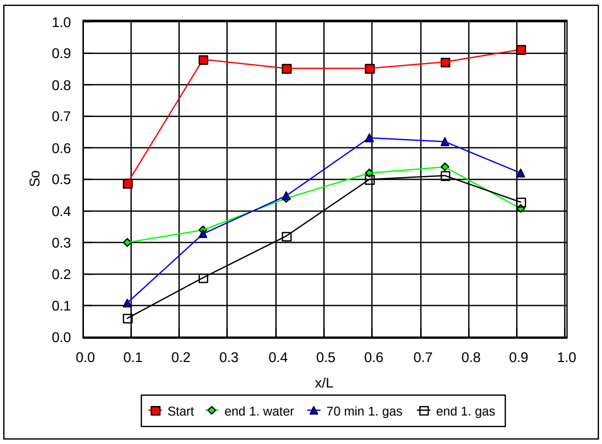

Fig. 8. Oil saturation during 1. water- and 1. gas flood in the WAG process.